

Curved QCD string dynamics

Theodore J. Allen

*Department of Physics, Eaton Hall
Hobart and William Smith Colleges
Geneva, New York 14456 USA*

M. G. Olsson

*Department of Physics, University of Wisconsin,
1150 University Avenue, Madison, Wisconsin 53706 USA*

Siniša Veseli

*Theoretical Physics Department
Fermi National Accelerator Laboratory
P.O. Box 500, Batavia, Illinois 60510 USA
(August 22, 2018)*

Abstract

We consider the effects of going beyond the approximation of a straight string in mesons by using a flexible flux tube model wherein a Nambu-Goto string bends in response to quark accelerations. The curved string is dynamically identical to the straight string even for ultra-relativistic mesons except for a small additional radial momentum. We numerically solve the curved string model in the case where both ends have equal mass quarks and also the case where one end is fixed. No approximation of non-relativistic motion is made. We note some small but interesting difference from the straight string.

I. INTRODUCTION

As the separation between quarks becomes large, their color field contracts into a string-like or flux tube configuration. QCD is thus thought to resemble string theory in the large distance regime. The Nambu-Goto-Polyakov QCD string [1] is an elegant model for this color field from which valuable insights on the nature of QCD are expected. The most obvious of these is the well known picture of static linear confinement. For a dynamical hadron the simplest assumption for the long distance color field configuration is that the flux tube/string always remains straight. This was the assumption of the relativistic flux tube model for mesons [2] which has enjoyed phenomenological success.

As pointed out by Nesterenko [3] such rigid string models cannot strictly be considered Nambu-Goto strings since the string cannot remain straight during dynamical motion of the quarks. Recently, the present authors [4] found an explicit solution to the string equations describing the deviation from straightness due to non-uniform end motion. The principal assumptions in our calculation are to treat the motion as “adiabatic” and that the deviation from straightness is small. The adiabatic assumption is just that the string shape depends on the end motion and that there is no other explicit time dependence. By direct calculation we find that for all physical cases the string never bends very much even for relativistic motion.

An interesting conclusion of our previous work [4] was that almost every dynamical quantity for the curved string is the same as the straight string. The angular momentum, energy, and momentum perpendicular to the line connecting the quarks are unchanged for small string deformations assuming the quark distance and angular velocity are the same for the curved and straight strings.

The sole difference between the dynamically curved string and the straight string is the component of momentum along the line connecting the quarks. From Fig. 1 the origin of this radial momentum is clear. It is also evident that the contribution from the outer part of the string will predominate due to the larger velocity of the end of the string. The net result will be an inward flowing radial momentum for the case shown in Fig. 1 corresponding to increasing angular velocity ($\dot{\omega} > 0$). For a meson the total angular momentum is conserved and hence if the angular velocity is increasing the distance between the quarks must be decreasing. We conclude that the tube radial momentum due to curvature always has the same sign as the quark’s radial momentum. In a meson with equal mass quarks the two halves of the string have equal but opposite radial momenta, just as the quarks do.

Since the curved string meson is nearly identical to the rigid (straight) string meson similar methods are indicated for our numerical solution. The effect of the curvature induced radial momentum is to shift the energy level solutions downward only a few MeV. For

practical purposes it is quite sufficient to ignore deviation from straightness even for massless quarks with resulting ultra-relativistic kinematics. A principal result thus is that one can use the simpler straight string approximation with negligible loss in accuracy.

The remainder of the paper is organized as follows. In Sec. II we start with the string plus quark action and establish the equations of motion and conserved quantities. The solution for the curved string is reviewed in Sec. III and the energy, angular momentum, and linear momentum are computed. We show here that the curvature of the string induced by general quark motion does not contribute to the energy and angular momentum. The sole effect of the curved string is to enhance the radial momentum of the quark. The method of quantization of the quark-string system and the solutions scheme is covered in Sec. IV. Our numerical results and general conclusions are given in Sections V and VI.

II. THE STRING-QUARK ACTION

We begin by reviewing the formalism of the Nambu-Goto-Polyakov [1,5] string and spinless quark actions and some expressions for conserved quantities. The action for a quark and anti-quark connected by a QCD string is

$$S = -\frac{a}{2} \int d\tau \int d\sigma \sqrt{-h} h^{ab} X_{,a}^{\mu} X_{,b}^{\nu} \eta_{\mu\nu} - \sum_{i=1,2} \int d\tau \left(m \sqrt{-\dot{x}^{\mu} \dot{x}_{\mu}} \right)_i, \quad (2.1)$$

where h^{ab} is the inverse of the two-dimensional metric h_{ab} whose indices run over τ and σ , while $h = \det(h_{ab})$. $X^{\mu}(\tau, \sigma)$ is the string position and $X_{,a}^{\mu} \equiv \partial_a X^{\mu}$. The two quark coordinates are $x_i^{\mu}(\tau) \equiv X^{\mu}(\tau, \sigma_i)$ at the ends of the string. We use the metric signature conventions that $h = (-, +)$ and $\eta = (-, +, +, +)$.

The action (2.1) is classically equivalent to the string tension a times the worldsheet area swept out by the string minus the masses of the quarks times their worldline lengths. Variation of the Lagrange multiplier h_{ab} determines that it is equal to the embedding metric, up to a multiplicative constant

$$h_{ab} = X_{,a}^{\mu} X_{,b}^{\nu} \eta_{\mu\nu}. \quad (2.2)$$

Variation of the string and quark positions yields the equations of motion

$$(\sqrt{-h} h^{ab} X_{,b}^{\mu})_{,a} = 0, \quad (2.3)$$

$$-(-)^i a \sqrt{-h} h^{\sigma b} X_{,b}^{\mu} = (p_i^{\mu})_{,\tau}, \quad (2.4)$$

where the canonical quark momenta are

$$p_i^\mu = \frac{\delta S_{\text{quark}}}{\delta \dot{x}_i^\mu} = \left(\frac{m \dot{x}^\mu}{\sqrt{-\dot{x}^\nu \dot{x}_\nu}} \right)_i \equiv (m\gamma \dot{x}^\mu)_i, \quad (2.5)$$

and $\dot{x}_i^\mu = (x_i^\mu)_{,\tau}$. The string momentum density is

$$\Pi_\mu(\tau, \sigma) = \frac{\delta S_{\text{string}}}{\delta \dot{X}^\mu} = -a\sqrt{-h} h^{\tau a} X_{\mu,a}(\tau, \sigma). \quad (2.6)$$

The total energy and momentum of the string-quark system then follows

$$P_{\text{total}}^\mu = P_{\text{string}}^\mu + P_{\text{quarks}}^\mu = \int_{\sigma_1}^{\sigma_2} \Pi^\mu(\tau, \sigma) d\sigma + \sum_{i=1,2} p_i^\mu, \quad (2.7)$$

and the system angular momentum is

$$J_{\text{total}}^{\mu\nu} = J_{\text{string}}^{\mu\nu} + J_{\text{quarks}}^{\mu\nu} = \int_{\sigma_1}^{\sigma_2} X^{[\mu} \Pi^{\nu]} d\sigma + \sum_{i=1,2} (x^{[\mu} p^{\nu]})_i. \quad (2.8)$$

Because of the spherical symmetry of the string and quarks system, we may consider motion in the (x^1, x^2) plane. It is useful then to use helicity coordinates

$$X^\pm = \frac{X^1 \pm iX^2}{\sqrt{2}}. \quad (2.9)$$

We will adopt the notation

$$\mathbf{X} \equiv X^+, \quad (2.10)$$

and therefore $\mathbf{X}^* = X^-$. In terms of the spatial coordinate \mathbf{X} , the above results become

$$h_{ab} = -X_{,a}^0 X_{,b}^0 + 2 \operatorname{Re}(\mathbf{X}_{,a}^* \mathbf{X}_{,b}), \quad (2.11)$$

$$E = P^0 = -a \int_{\sigma_1}^{\sigma_2} d\sigma \sqrt{-h} h^{\tau a} X_{,a}^0 + \sum_{i=1,2} (m\gamma)_i. \quad (2.12)$$

The spatial momentum can be expressed in helicity form as

$$\begin{aligned} \mathbf{P} &= \frac{1}{\sqrt{2}} (P^1 + iP^2) \\ &= -a \int_{\sigma_1}^{\sigma_2} d\sigma \sqrt{-h} h^{\tau a} \mathbf{X}_{,a} + \sum_{i=1,2} (m\gamma \dot{\mathbf{x}})_i, \end{aligned} \quad (2.13)$$

where the quark coordinate $\mathbf{x}_i(\tau)$ is

$$\mathbf{x}_i(\tau) = \mathbf{X}(\tau, \sigma_i). \quad (2.14)$$

Similarly, the angular momentum J^3 perpendicular to the plane of motion is

$$J^3 = 2a \int_{\sigma_1}^{\sigma_2} d\sigma \sqrt{-h} h^{\tau b} \operatorname{Im}(\mathbf{X}_{,b}^* \mathbf{X}) + 2 \sum_{i=1,2} (m\gamma \operatorname{Im}(\dot{\mathbf{x}}^* \mathbf{x}))_i. \quad (2.15)$$

III. THE CURVED STRING WITH ONE FIXED END

As we showed previously, it is possible to perturb about an exact straight string solution to obtain the shape of a string in which one end is fixed and the other has a sufficiently small angular acceleration. The string motion in a meson can be considered as a special case where the system angular momentum and energy are conserved. We begin this section by re-establishing this result by an abbreviated method. In [4] we began with the ansatz

$$\begin{aligned} X^0(\tau, \sigma) &= \tau = t, \\ \mathbf{X}(\tau, \sigma) &= \frac{1}{\sqrt{2}}(\sigma R(t) + F(\sigma)) \exp[i(\omega t + \phi(t))], \end{aligned} \quad (3.1)$$

where $F(\sigma)$ is complex and $F(\sigma)$ and $\phi(t)$ are small. A more convenient starting point can be found by observing that if $X(t, \sigma = 1) \equiv \frac{R}{\sqrt{2}}$, reparametrization invariance allows us to set $\text{Re}(F) = 0$. We can then exploit the assumption of small deviation from straightness to make the simpler but related ansatz

$$\begin{aligned} X^0(\tau, \sigma) &= \tau = t, \\ \mathbf{X}(\tau, \sigma) &= \frac{1}{\sqrt{2}}\sigma R(t) \exp(i\Phi), \end{aligned} \quad (3.2)$$

where the overall phase is a rigid rotation plus the sum of two phases, each dependent upon only one of the coordinates

$$\Phi = \omega t + \phi(t) + f(\sigma). \quad (3.3)$$

With X^μ of the above form, from Eq. (2.11) we see that the worldsheet metric is given as

$$h_{ab} = -\delta_{at}\delta_{tb} + (\sigma R)_{,a}(\sigma R)_{,b} + (\sigma R)^2 \Phi_{,a}\Phi_{,b}, \quad (3.4)$$

with individual components

$$h_{tt} = -\gamma^{-2}(\sigma) + 2\sigma^2 R^2 \omega \dot{\phi}, \quad (3.5)$$

$$h_{t\sigma} = \sigma R \dot{R} + \sigma^2 R^2 \omega f', \quad (3.6)$$

$$h_{\sigma\sigma} = R^2, \quad (3.7)$$

and volume density

$$\sqrt{-h} = \sqrt{-\det h_{ab}} = \frac{R}{\gamma_\perp(\sigma)} \left(1 - 2\sigma^2 R^2 \gamma_\perp^2(\sigma) \omega \dot{\phi}\right). \quad (3.8)$$

In the above expressions we have used the notation

$$\gamma_\perp^{-2}(\sigma) = 1 - \sigma^2 \omega^2 R^2, \quad (3.9)$$

$$\gamma^{-2}(\sigma) = \gamma_\perp^{-2}(\sigma) - \sigma^2 \dot{R}^2. \quad (3.10)$$

The equations of motion for the string (2.3) hold both for the temporal $X^0 = t$ and spatial X components. In the case of X^0 , we have, to first order in f and ϕ

$$\left[\gamma_{\perp}(\sigma) + \gamma_{\perp}^3(\sigma) \sigma^3 \omega \dot{\phi} \right]_{,t} = \left[\gamma_{\perp}(\sigma) \sigma \dot{R} + \gamma_{\perp}(\sigma) \sigma^2 R \omega f' \right]_{,\sigma}. \quad (3.11)$$

Using the easily verified identity $(\gamma_{\perp}(\sigma) R)_{,t} = \dot{R}(\sigma \gamma_{\perp}(\sigma))_{,\sigma}$, and dropping $\dot{R} \dot{\phi}$ terms, we reduce Eq. (3.11) to

$$\frac{d}{d\sigma} \left(\sigma^2 \gamma_{\perp}(\sigma) \frac{df}{d\sigma} \right) = R^2 \dot{\omega} \sigma^2 \gamma_{\perp}^3(\sigma). \quad (3.12)$$

Here we introduce the notation $\dot{\omega} \equiv \ddot{\phi}$. It can be shown [4] that the equations of motion for the spatial coordinate X^i also reduce to this same equation. Integration of Eq. (3.12) yields

$$\frac{df}{d\sigma} = \frac{R^2 \dot{\omega}}{v_{\perp}^2} \left[\sigma - \frac{\arcsin \sigma v_{\perp}}{\sigma^2 \gamma_{\perp}(\sigma)} \right] + C_1 \frac{1}{\sigma^2 \gamma_{\perp}(\sigma)}, \quad (3.13)$$

whose solution is

$$\begin{aligned} \sigma f(\sigma) &= \frac{\dot{\omega} R^2}{v_{\perp}^3} \left[\frac{1}{2} \sigma v_{\perp} \arcsin \sigma v_{\perp} \right] \arcsin \sigma v_{\perp} \\ &+ C_1 \sigma v_{\perp} + C_2 \left(\sqrt{1 - \sigma^2 v_{\perp}^2} + \sigma v_{\perp} \arcsin \sigma v_{\perp} \right). \end{aligned} \quad (3.14)$$

In the above we have defined the transverse end velocity $v_{\perp} \equiv \omega R$. After removal of the rigidly rotating phase, the string coordinate can be written in terms of a radial and a transverse piece

$$\mathbf{X} = \frac{1}{\sqrt{2}} (X_R + i X_{\perp}), \quad (3.15)$$

which are given by

$$\frac{X_R}{R} = \sigma, \quad (3.16)$$

$$\frac{X_{\perp}}{R} = \sigma f(\sigma) \equiv \frac{1}{6} \dot{\omega} R^2 \text{shape}(\sigma, v_{\perp}). \quad (3.17)$$

Imposing the end conditions $X_{\perp}(\sigma = 0) = X_{\perp}(\sigma = 1) = 0$, we find

$$\begin{aligned} \text{shape}(\sigma, v_{\perp}) &= -\frac{6}{v_{\perp}^3} \left[\frac{1}{2} \sigma v_{\perp} \left((\arcsin v_{\perp})^2 - (\arcsin \sigma v_{\perp})^2 \right) \right. \\ &\left. + \sigma \sqrt{1 - v_{\perp}^2} \arcsin v_{\perp} - \sqrt{1 - \sigma^2 v_{\perp}^2} \arcsin \sigma v_{\perp} \right]. \end{aligned} \quad (3.18)$$

The string shape for $v_{\perp} \ll 1$ is shown in Fig. 1. Other examples are shown in Ref. [4].

As we pointed out earlier, one can compare the angular momentum, energy and linear momentum of the curved and straight string. The results are

$$J_{\text{curved}}^3 = J_{\text{straight}}^3 = \frac{aR^2}{2v_{\perp}} \left[\frac{\arcsin(v_{\perp})}{v_{\perp}} - \sqrt{1 - v_{\perp}^2} \right], \quad (3.19)$$

$$E_{\text{curved}} = E_{\text{straight}} = aR \frac{\arcsin v_{\perp}}{v_{\perp}}, \quad (3.20)$$

$$P_{\perp \text{curved}} = P_{\perp \text{straight}} = \frac{aR}{v_{\perp}} \left[1 - \sqrt{1 - v_{\perp}^2} \right]. \quad (3.21)$$

Although there is no radial tube momentum for the straight string, it is non-zero for the curved string. This is evident from Fig. 1 and by direct calculation

$$P_R = -aR \frac{\dot{\omega} R^2}{v_{\perp}^4} \left[1 - \sqrt{1 - v_{\perp}^2} - \frac{v_{\perp}}{2} \arcsin v_{\perp} \right] \arcsin v_{\perp}. \quad (3.22)$$

The presence of radial string momentum is the only dynamical evidence of the curved string.

We have considered so far in this section only the heavy-light meson case where one tube end is fixed. Although the general straight string case was discussed previously [2] we will consider here the generalization to curved strings of the equal quark mass case. In Fig. 2 we show the shape function from $-1 \leq \sigma \leq +1$ which describes the equal mass case. It is evident that we may immediately find the angular momentum, energy, and linear momentum from the preceding expressions by using the substitution

$$\begin{aligned} R &\rightarrow r/2, \\ v_{\perp} = \omega R &\rightarrow v_{\perp} = \omega r/2, \end{aligned} \quad (3.23)$$

which leads to the following expressions for the equal quark mass case

$$J_{\text{equal mass}}^3 = \frac{ar^2}{4v_{\perp}} \left[\frac{\arcsin v_{\perp}}{v_{\perp}} - \sqrt{1 - v_{\perp}^2} \right], \quad (3.24)$$

$$E_{\text{equal mass}} = ar \frac{\arcsin v_{\perp}}{v_{\perp}}, \quad (3.25)$$

$$P_r = -ar \frac{\dot{\omega} r^2}{8v_{\perp}^4} \left[1 - \sqrt{1 - v_{\perp}^2} - \frac{v_{\perp}}{2} \arcsin v_{\perp} \right] \arcsin v_{\perp}. \quad (3.26)$$

Again we note that E and J^3 for the straight and curved strings are identical. In the above we increased E and J^3 by a factor of two because of the two string pieces. Of course we must add the quark contribution to each quantity to obtain the total.

IV. QUANTIZATION AND METHOD OF NUMERICAL SOLUTION

We begin by reviewing the quantization of the classical expressions for the heavy-light straight string. From (2.13), (3.19) and (2.12), (3.20) the angular momentum and energy are

$$J^3 \equiv J = m\gamma v_\perp R + aR^2 F(v_\perp), \quad (4.1)$$

$$E = M_Q + m\gamma + aR \frac{\arcsin v_\perp}{v_\perp}, \quad (4.2)$$

where M_Q is the heavy quark mass and $F(v_\perp)$ is defined as

$$F(v_\perp) = \frac{1}{2v_\perp} \left(\frac{\arcsin v_\perp}{v_\perp} - \sqrt{1 - v_\perp^2} \right). \quad (4.3)$$

In the above $v_\perp = \omega R$ and we have used the notation

$$\gamma_\perp = \frac{1}{\sqrt{1 - v_\perp^2}}, \quad (4.4)$$

$$\gamma = \frac{1}{\sqrt{1 - v_\perp^2 - \dot{R}^2}}. \quad (4.5)$$

The radial quark velocity \dot{R} has to be eliminated in favor of the radial quark momentum by the relation

$$(p_R^{\text{quark}})^2 + m^2 = m^2 \left(\frac{\dot{R}^2}{1 - v_\perp^2 - \dot{R}^2} + 1 \right) = \frac{(m\gamma)^2}{\gamma_\perp^2}, \quad (4.6)$$

which leads to

$$m\gamma = W_R \gamma_\perp, \quad (4.7)$$

$$W_R = \sqrt{(p_R^{\text{quark}})^2 + m^2}. \quad (4.8)$$

From (4.1), (4.2), and (4.7) we have

$$\frac{J}{R} = W_R \gamma_\perp v_\perp + aR F(v_\perp), \quad (4.9)$$

$$E = M_Q + W_R \gamma_\perp + aR \frac{\arcsin v_\perp}{v_\perp}. \quad (4.10)$$

The above equations can be quantized [2] by making the replacements

$$J \rightarrow \sqrt{\ell(\ell + 1)}, \quad p_R^2 \rightarrow -\frac{1}{R} \frac{\partial^2}{\partial R^2} R, \quad (4.11)$$

and by symmetrizing terms which depend on both R and v_\perp with anticommutators ($\{A, B\} \equiv AB + BA$). This procedure leads to the following quantum-mechanical equation for the angular momentum and the energy

$$\frac{\sqrt{\ell(\ell+1)}}{R} = \frac{1}{2}\{W_R, \gamma_\perp v_\perp\} + a\{R, F(v_\perp)\} , \quad (4.12)$$

$$H = M_Q + \frac{1}{2}\{W_R, \gamma_\perp\} + \frac{a}{2}\left\{R, \frac{\arcsin v_\perp}{v_\perp}\right\} . \quad (4.13)$$

As we have shown in [4], the only difference between the straight and the curved QCD string is that the later has radial momentum,

$$p_R^{\text{tube}} = -aR(\dot{\omega}R^2)g(v_\perp) , \quad (4.14)$$

where we defined

$$g(v_\perp) = \left(1 - \sqrt{1 - v_\perp^2} - \frac{v_\perp}{2} \arcsin v_\perp\right) \frac{\arcsin v_\perp}{v_\perp^4} . \quad (4.15)$$

Since $p_R^{\text{quark}} = p_R - p_R^{\text{tube}}$, Eq. (4.8) then becomes,

$$W_R = \sqrt{(p_R - p_R^{\text{tube}})^2 + m^2} . \quad (4.16)$$

In order to quantize the above expressions it is convenient to write

$$\begin{aligned} \dot{\omega}R^2 &= \dot{v}_\perp R - \dot{R}v_\perp \\ &= \frac{1}{2}\left(\{\dot{v}_\perp, R\} - \{\dot{R}, v_\perp\}\right) . \end{aligned} \quad (4.17)$$

After promoting v_\perp and R to quantum-mechanical operators in (4.17) we can use the quantum dynamical equations of motion

$$\dot{v}_\perp = -i[v_\perp, H] , \quad (4.18)$$

$$\dot{R} = -i[R, H] , \quad (4.19)$$

which completely specifies the quantum version of $\dot{\omega}R^2$ in terms of R , v_\perp , and Hamiltonian given in (4.13), and allows us to quantize p_R^{tube} by choosing appropriate symmetrization between the non-commuting operators. This procedure gives us

$$p_R^{\text{tube}} = -a \frac{1}{2} \left\{ \dot{\omega}R^2, \frac{1}{2}\{R, g(v_\perp)\} \right\} . \quad (4.20)$$

The final step in quantizing (4.16) is to expand $(p_R - p_R^{\text{tube}})$ by writing

$$(p_R - p_R^{\text{tube}})^2 = p_R^2 - \{p_R, p_R^{\text{tube}}\} + (p_R^{\text{tube}})^2 . \quad (4.21)$$

Here, $p_R = -\frac{i}{R} \frac{\partial}{\partial R} R$ and p_R^{tube} is defined by (4.17) through (4.20).

The solution method for the straight string equations is discussed in detail in Ref. [2]. The fundamental problem is that the unknown operator v_\perp cannot be analytically eliminated, so one must eliminate it numerically. This can be accomplished by expanding the radial wave function in terms of a complete set of basis states, which reduces (4.12) to a transcendental infinite dimensional matrix equation. By truncating the number of the basis states to a finite number N , the matrix equation becomes finite dimensional, and can be solved by iteration procedure described in [2]. Once the matrix for v_\perp is known, one can calculate the Hamiltonian matrix from (4.13) and solve for the energy eigenvalues and corresponding wave functions. The modified algorithm for solving the curved string equations involves continually updating the W_R matrix during the iteration procedure [2] in which the matrix v_\perp is found.

Note that truncation introduces the dependence of the eigenvalues on the variational parameter β describing the basis states. However, if a sufficiently large number of basis states are used, this dependence will exhibit a ‘‘plateau’’ indicating a stable solution. Examples of this will be shown in Sec. V.

The equal quark mass meson can be quantized by a simple modification of the above. In this case we start with Eqs. (3.24)-(3.26) to obtain expressions analogous to (4.12), (4.13), and (4.20)

$$\frac{\sqrt{\ell(\ell+1)}}{r} = \{W_r, \gamma_\perp v_\perp\} + \frac{a}{4} \{r, F(v_\perp)\} , \quad (4.22)$$

$$H = \{W_r, \gamma_\perp\} + \frac{a}{2} \left\{ r, \frac{\arcsin v_\perp}{v_\perp} \right\} , \quad (4.23)$$

$$p_r^{\text{tube}} = -\frac{a}{16} \left\{ \dot{\omega} r^2, \frac{1}{2} \{r, g(v_\perp)\} \right\} . \quad (4.24)$$

The numerical solution is step by step the same as for the heavy-light case.

The more general case of unequal arbitrary masses at the ends is one step more involved. This case was solved in [2] for the straight string. For mesons with unequal mass quarks, one must require that $P_\perp^{\text{tot}} \equiv 0$. This is equivalent to solving for the center of momentum in addition to the angular momentum and energy equations. The curved string dynamical solution should proceed similarly to the two special cases discussed previously.

V. NUMERICAL RESULTS

For zero angular momentum states we observe from (4.12) and (4.22) that $v_\perp = 0$ as expected. The tube radial momentum is zero and the Hamiltonians (4.13) and (4.23) become

equivalent to “spinless Salpeter” equations, which have well defined numerical solutions [2]. We will therefore confine ourselves to non-zero angular momenta.

The results for equal mass and heavy-light mesons are qualitatively similar and we will discuss these string configurations in parallel, pointing out the similarities and differences. As mentioned in the preceding section the set of basis states have a scale parameter β . For a given truncation to N basis states it is customary to plot energy eigenvalues as a function of β to identify a “plateau” indicating a stable solution. In Fig. 3 (heavy-light) and Fig. 4 (equal mass) we show the β dependence of the excitation energy of the p -wave ground state meson with massless light quarks. The energy calculation is done twice; first with the straight string model and then with the curved string. We note that as the number of basis states increases definite plateaus develop.

The second observation we make from Figs. 3 and 4 is that the curved string energy is slightly less than the straight string energy. We believe this results from the reduction of the effective string tension due to the transverse motion of the string during the quark’s motion. The difference in the p -wave case, shown in Fig. 3, is just a few MeV but this varies with angular momentum and radial excitation.

In Figs. 5 and 6 we illustrate how the curved and straight string differ for a variety of low lying states. The cases shown are for zero mass light quark(s) at the end(s) of the string. The general trend is that the difference increases from zero at $\ell = 0$ (which must be the case) to about $15 MeV$ at the higher angular momentum values shown.

The dependence of the energy difference for p -wave solutions on the mass of the quark at either end of the string is illustrated in Fig. 7 (heavy-light) and Fig. 8 (equal mass). The energy difference ΔE is seen to decrease rapidly as the quark mass increases. As expected, the curvature effect on the solution is largest for massless quarks.

Finally, in Fig. 9 we show the Regge pattern for the curved string with one massless quark and the other end fixed. We exhibit the corresponding Regge pattern for massless quark ends in Fig. 10. On this scale they are similar to those of the straight string. One observes towers of nearly degenerate states of even (or odd) angular momentum. The two cases are analogous except that the heavy-light Regge slope is double the light-light slope. Except for the value of the slope, this pattern is very similar to that of scalar potential confinement [6,7].

VI. CONCLUSION

In this paper we have investigated the dynamical effects of the small radial momentum developed by a QCD string as it bends in response to the angular acceleration of the quarks on the ends. Our principal results are that one can successfully implement the curved string

solutions into a dynamical meson model with massive quarks at the string ends. The solution is self-consistent in that for a physical state the deviation from straightness is small. For such small transverse string motion the energy, angular momentum, and transverse momentum are identical to those of a straight string with the same angular velocity. When the small curvature induced radial momentum is incorporated into the numerical method one finds solutions that are very similar to those of the straight string.

The curvature effects are largest for massless quarks. Even in this case one finds shifts of at most a few MeV . Our results indicate that for most purposes the simpler straight string model gives nearly correct results and if desired, more accuracy can be readily achieved.

ACKNOWLEDGMENTS

This work was supported in part by the US Department of Energy under Contract No. DE-FG02-95ER40896. Fermilab is operated by URA under DOE contract DE-AC02-76CH03000.

REFERENCES

- [1] Y. Nambu, “*Quark model and the factorization of the Veneziano Amplitude,*” in *Symmetries and quark models*, ed. R. Chand, (Gordon and Breach, 1970); T. Goto, *Prog. Theor. Phys.* **46**, 1560 (1971); L. Susskind, *Nuovo Cimento* **69A**, 457 (1970); A.M. Polyakov, *Phys. Lett.* **103B**, 207 (1981).
- [2] M.G. Olsson and S. Veseli, *Phys. Rev. D* **51**, 3578 (1995). This paper contains many references to previous work.
- [3] V.V. Nesterenko, *Z. Phys. C* **47**, 111 (1990).
- [4] T.J. Allen, M.G. Olsson, and S. Veseli, hep-ph/9810363, *Phys. Rev. D* (in press).
- [5] B.M. Barbashov and V.V. Nesterenko, “*Introduction to the relativistic string theory,*” (World Scientific, 1990).
- [6] M.G. Olsson, *Phys. Rev. D* **55**, 5475 (1997).
- [7] M.G. Olsson, S. Veseli, K. Williams, *Phys. Rev. D* **51**, 5079 (1995).

FIGURES

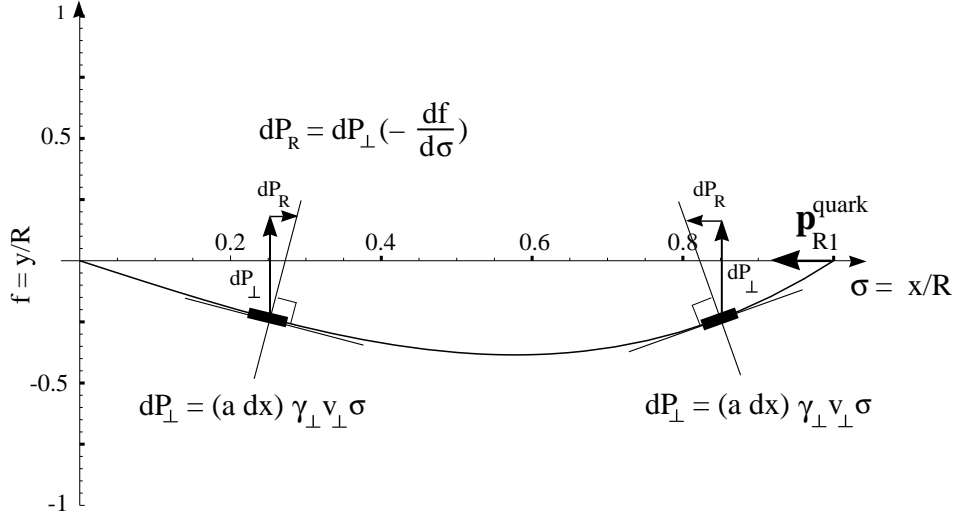


FIG. 1. The solution to the string shape (3.17) with positive $\dot{\omega}$ and $v_{\perp} \ll 1$. The transverse and radial momenta of two elements are depicted. The contribution at the larger radius will predominate giving a net radial momentum parallel to the quark’s radial momentum.

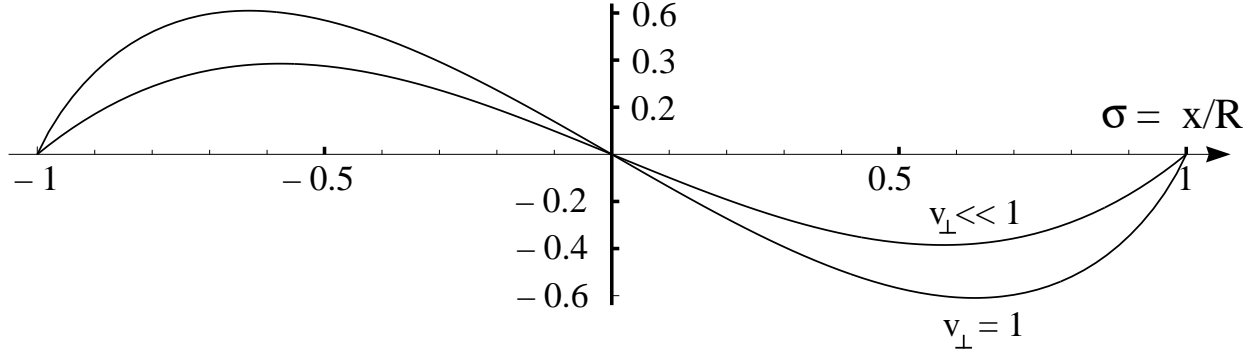


FIG. 2. The solution to the string shape (3.17) with positive $\dot{\omega}$ for a string with equal mass quarks at its ends. The “shape function” (3.18) is shown for non-relativistic and ultra-relativistic quark rotation.

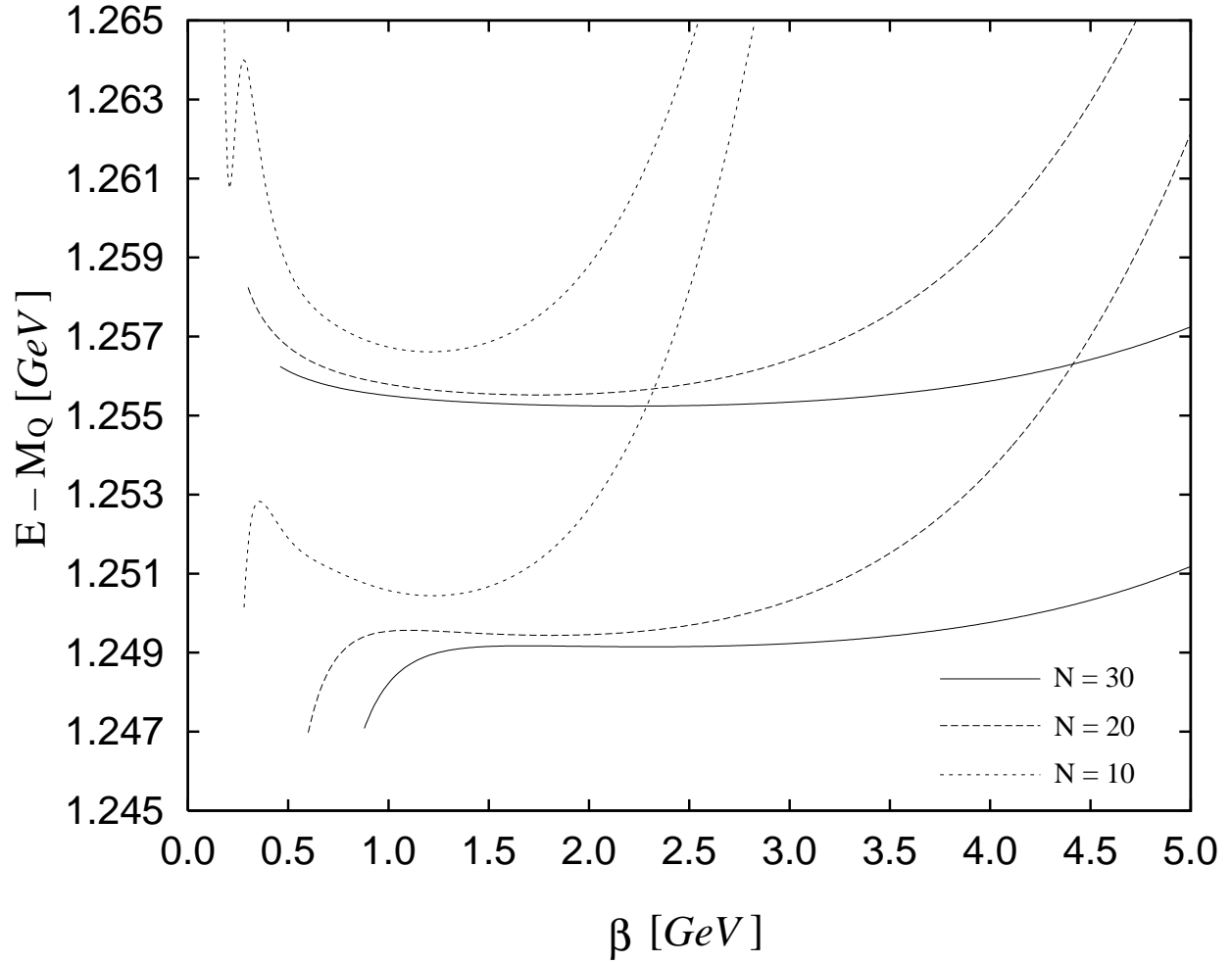


FIG. 3. Dependence on the variational parameter β of the ground state p -wave excitation energy of the heavy-light Hamiltonian with the straight string (upper curves) and with the curved string (lower curves). We used $a = 0.2 \text{ GeV}^2$ and light quark mass $m = 0$. Results shown were obtained with 10, 20 and 30 basis states.

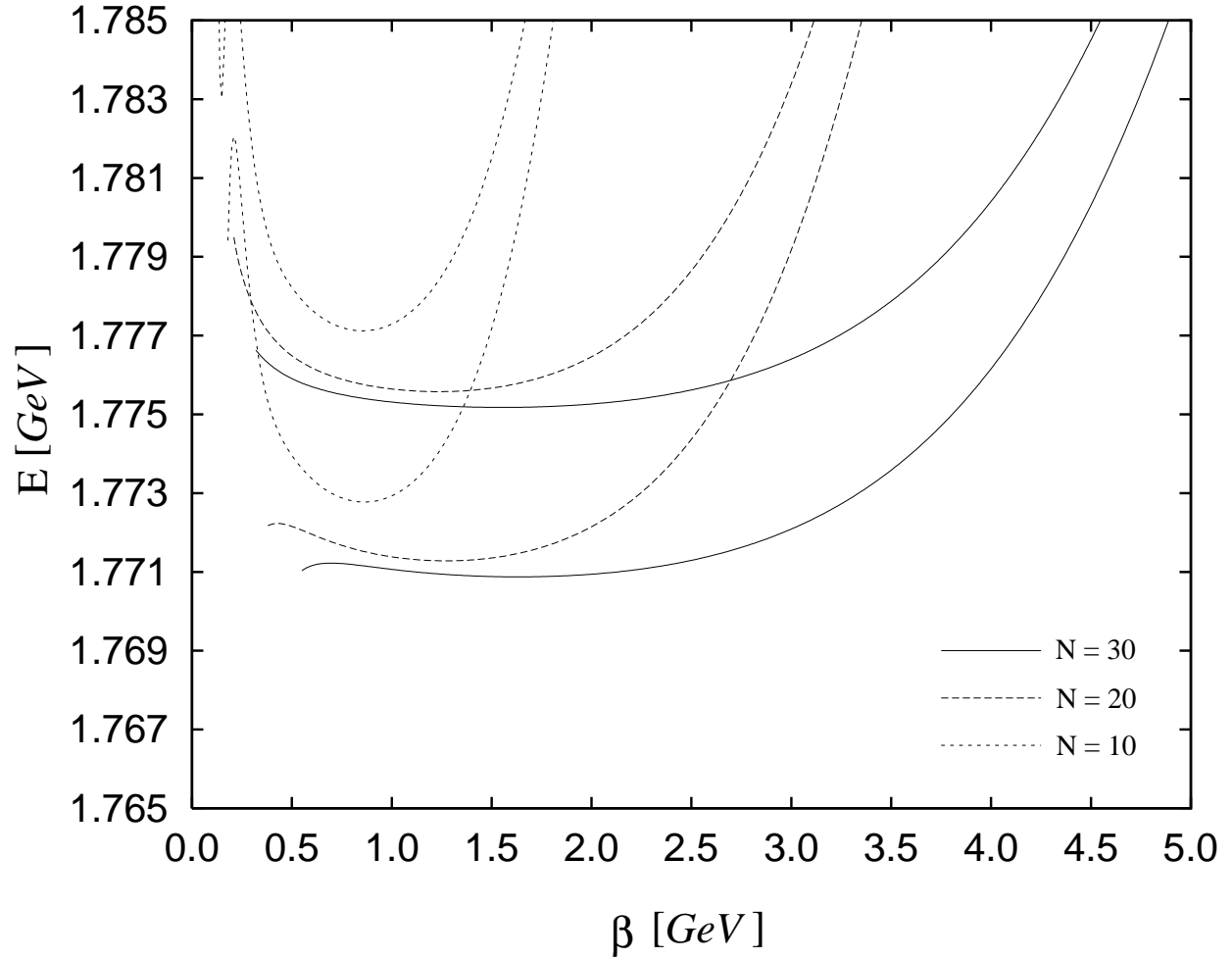


FIG. 4. Dependence on the variational parameter β of the ground state p -wave excitation energy of the equal mass Hamiltonian with the straight string (upper curves) and with the curved string (lower curves). We used $a = 0.2 \text{ GeV}^2$ and quark mass $m = 0$. Results shown were obtained with 10, 20 and 30 basis states.

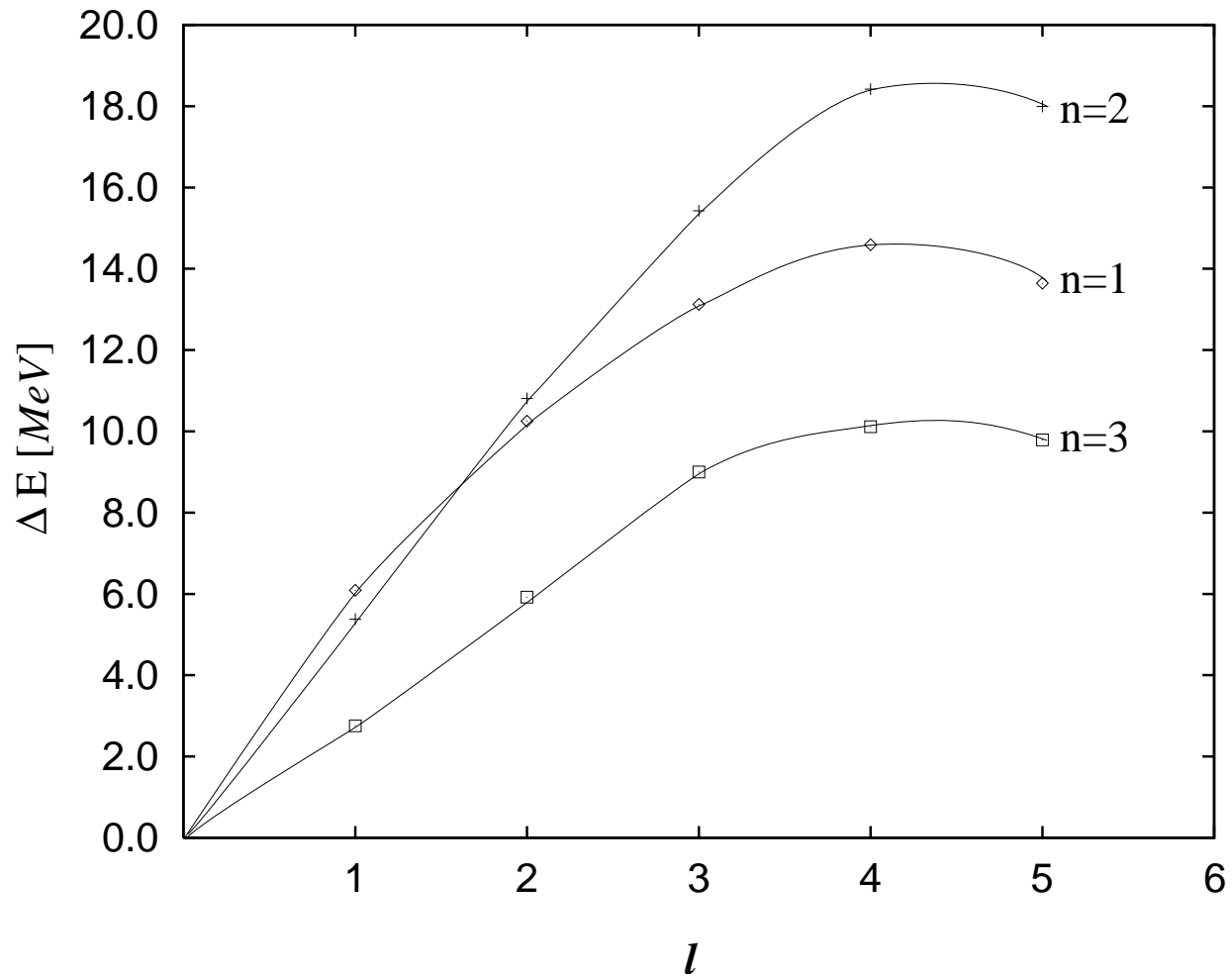


FIG. 5. Difference between the energies of the straight and curved heavy-light Hamiltonian as a function of the orbital angular momentum. We used $a = 0.2 \text{ GeV}^2$ and light quark mass $m = 0$. Results shown are for the ground state ($n = 1$) and for the first two radially excited states.

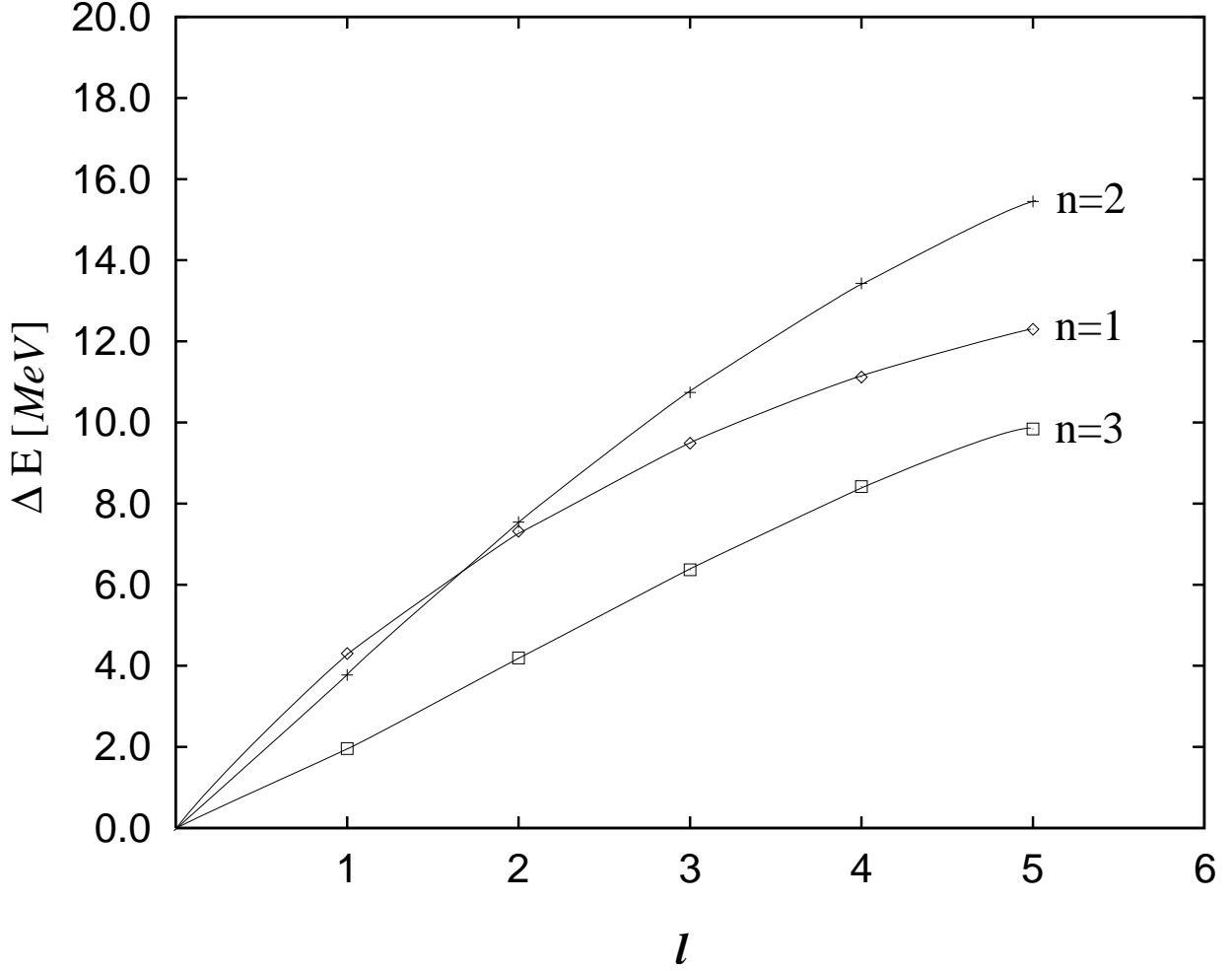


FIG. 6. Difference between the energies of the straight and curved equal mass Hamiltonian as a function of the orbital angular momentum. We used $a = 0.2 \text{ GeV}^2$ and light quark mass $m = 0$. Results shown are for the ground state ($n = 1$) and for the first two radially excited states.

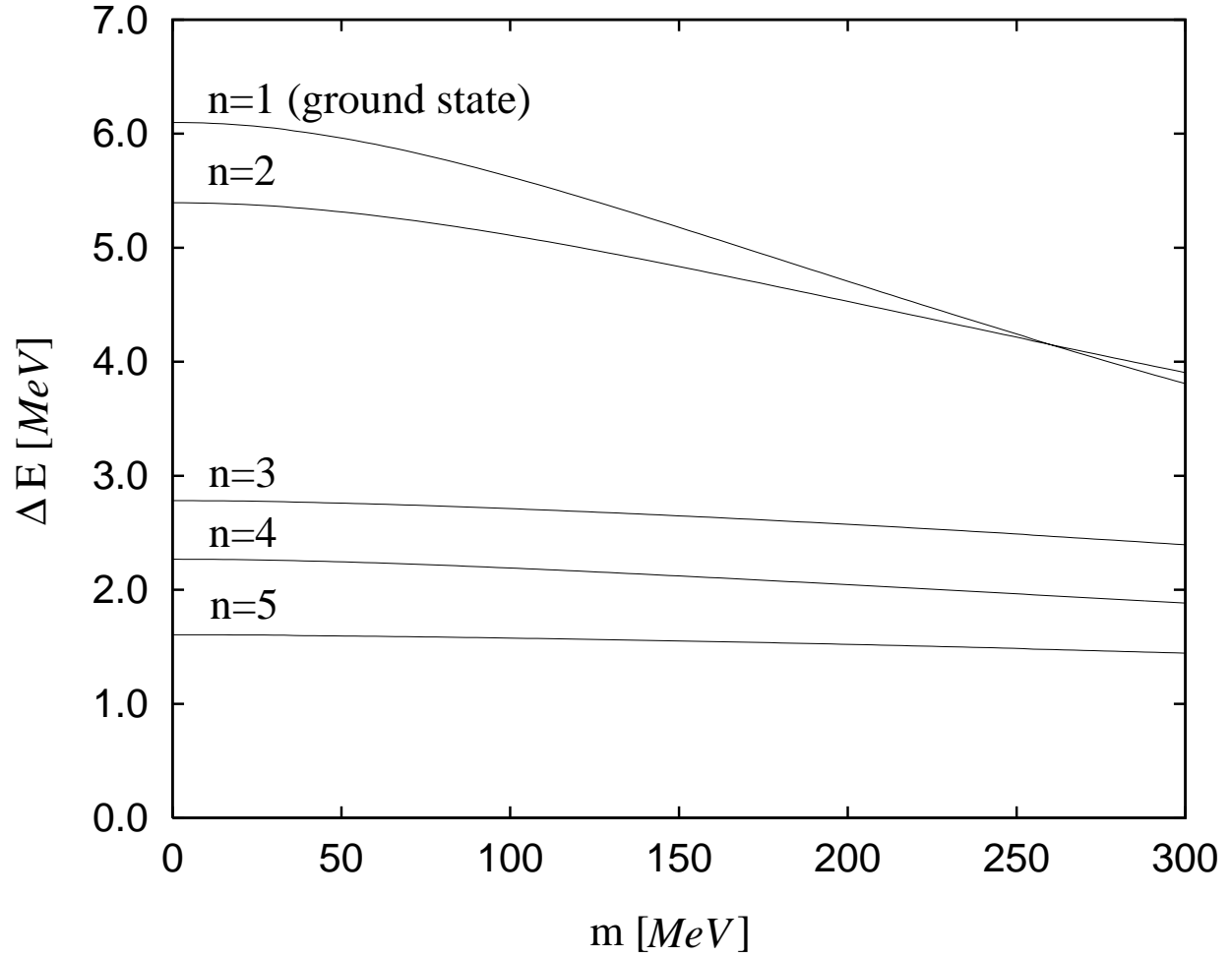


FIG. 7. Difference between the p -wave ($\ell = 1$) energies of the straight and curved heavy-light Hamiltonian as a function of the light quark mass. We used $a = 0.2 \text{ GeV}^2$, and results shown are for the ground state ($n = 1$) and for the first four radially excited states.

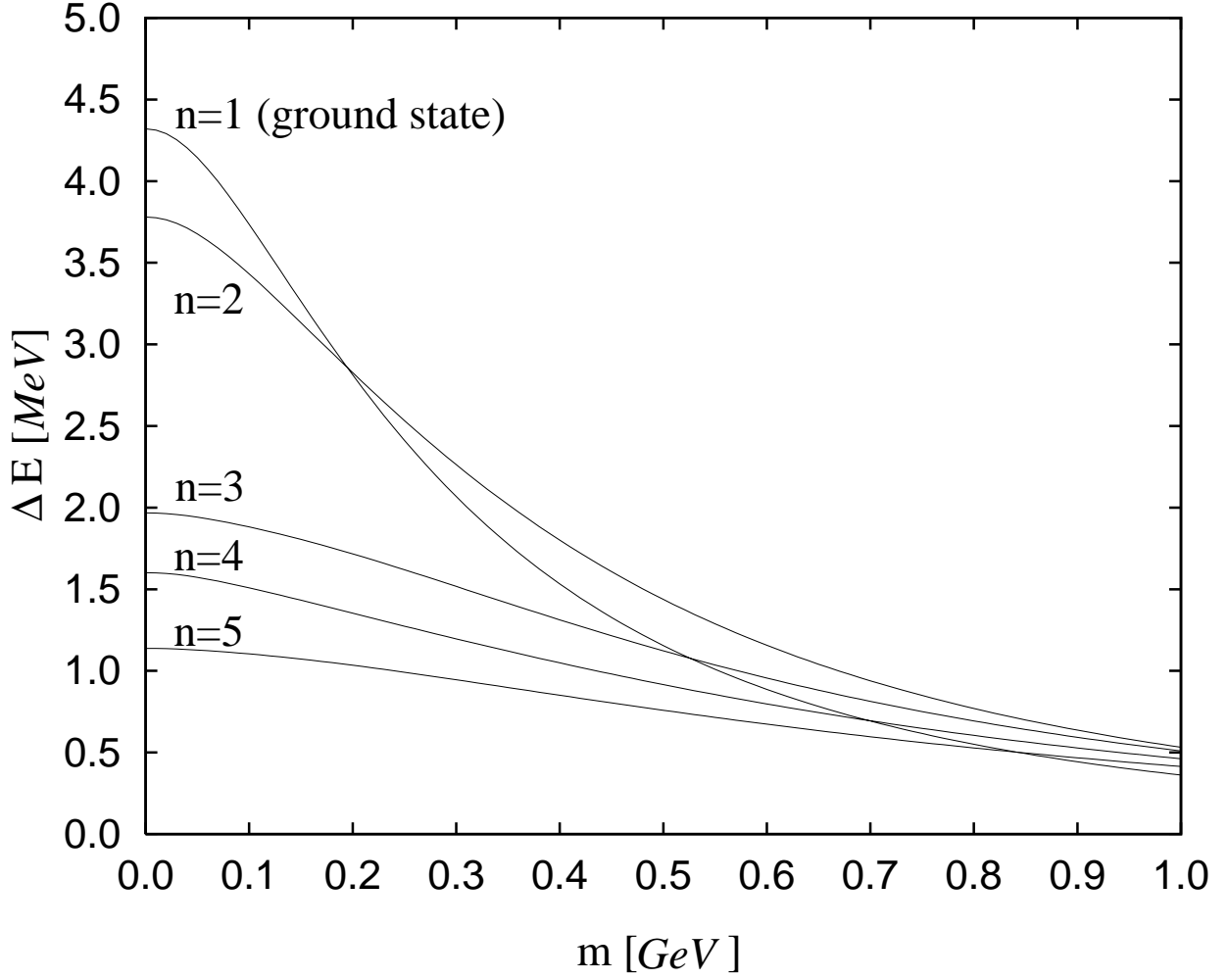


FIG. 8. Difference between the p -wave ($\ell = 1$) energies of the straight and curved equal-mass Hamiltonian as a function of the quark mass. We used $a = 0.2 \text{ GeV}^2$, and results shown are for the ground state ($n = 1$) and for the first four radially excited states.

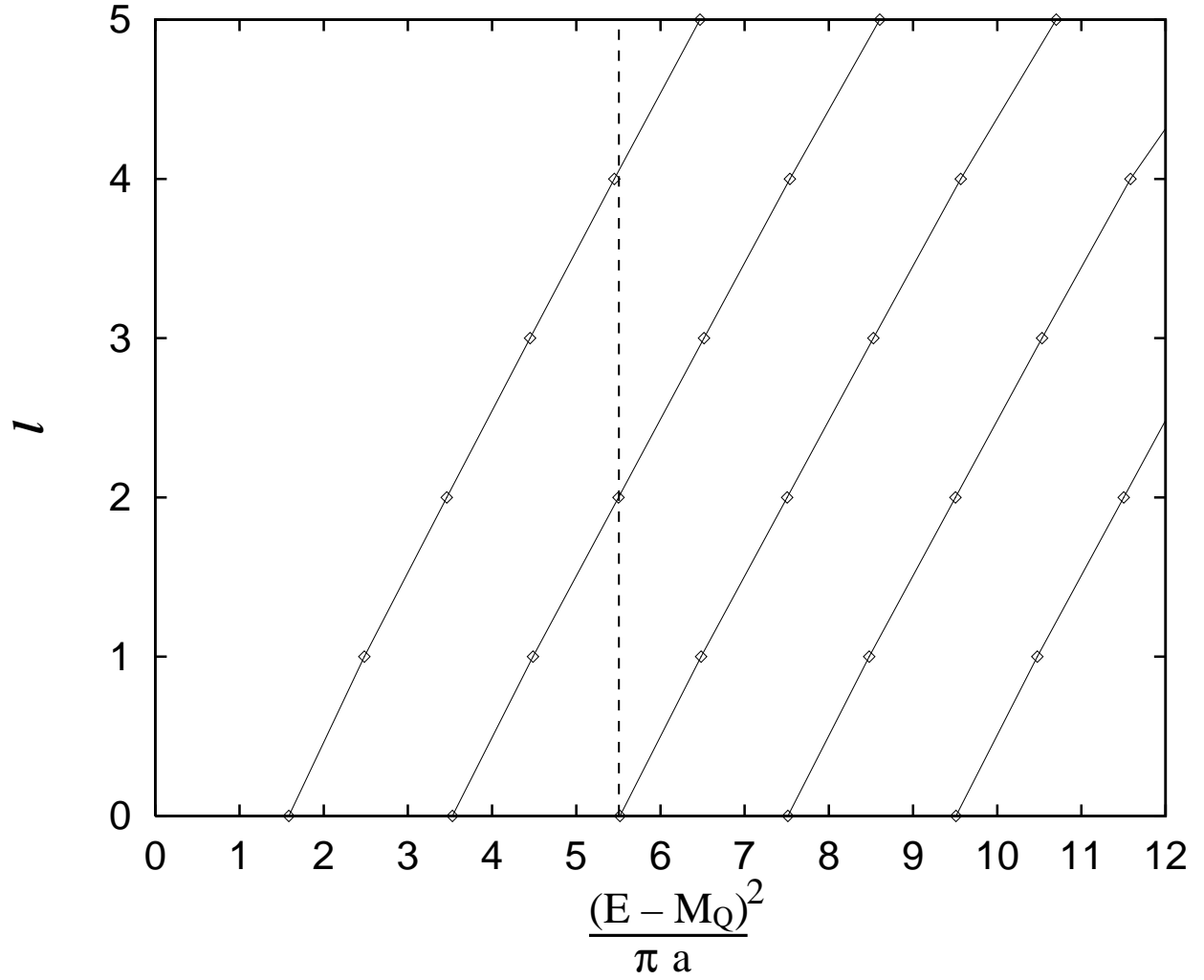


FIG. 9. Regge trajectories for the heavy-light Hamiltonian with the curved string having a massless quark. The vertical line illustrates the tower structure of nearly degenerate states of alternating angular momentum.

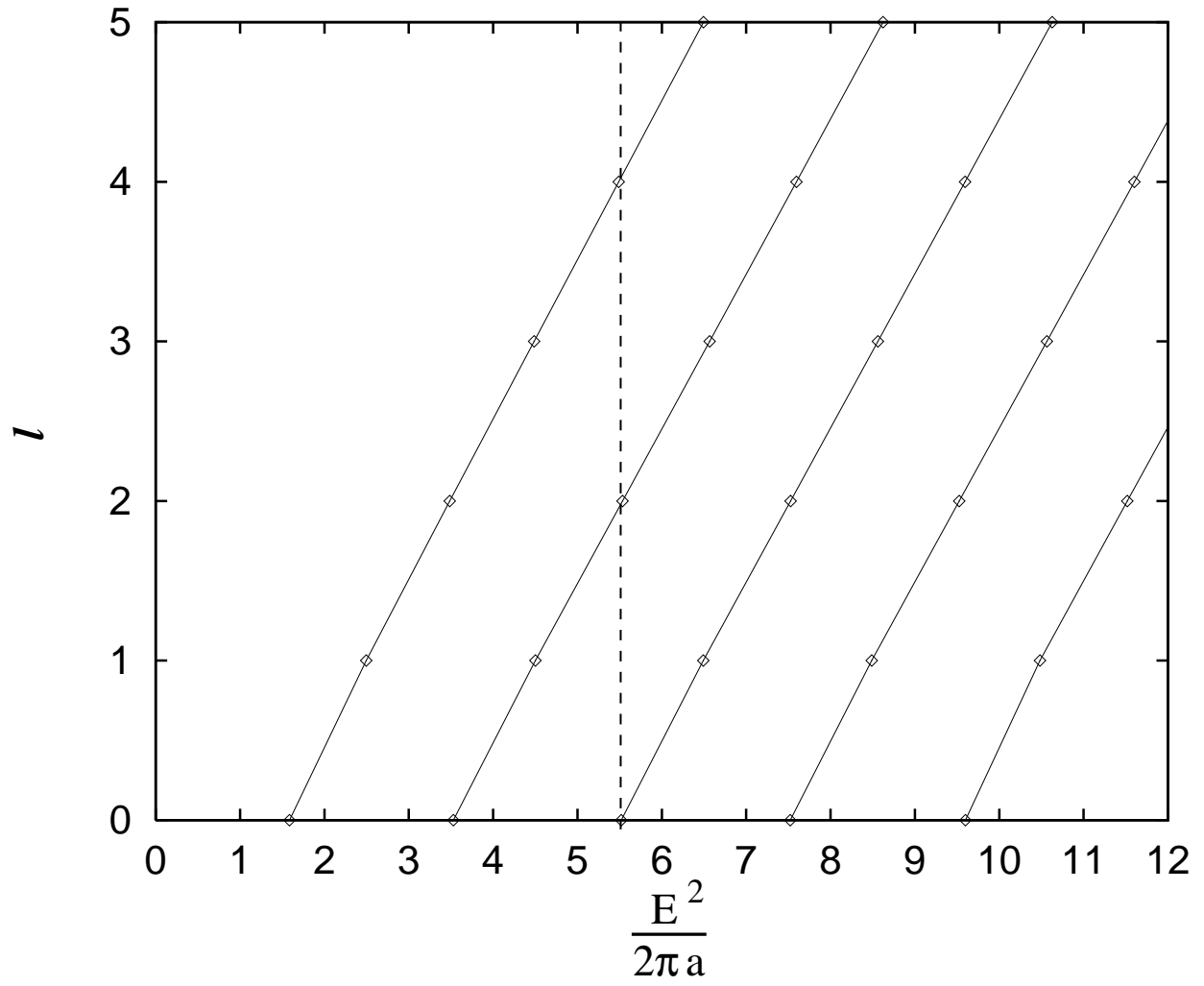


FIG. 10. Regge trajectories for the equal-mass Hamiltonian with the curved string having massless quarks at its ends. The vertical line illustrates the tower structure of nearly degenerate states of alternating angular momentum.